Improving Near-URLLC Services Performance over Multi-Hop Topologies in DECT-2020 NR Systems

Roman Glazkov[1], Andrey Samuylov[1], Anna Gaydamaka[1] Dmitri Moltchanov[1], Juho Pirskanen[2], Jussi Numminen[2], Mikko Valkama[1]
[1]Unit of Electrical Engineering, Tampere University, Finland
[2] Wirepas Oy, Tampere, Finland
✉ Contact author's e-mail: roman.glazkov@tuni.fi

***Abstract*—DECT-2020 NR is a radio access technology designed for 5G Internet of Things (IoT) applications. By leveraging multi-hop communications and listen-before-talk (LBT) mechanisms, DECT-2020 NR offers a flexible and cost-effective deployment solution for massive machine-type communications (mMTC). The ETSI standardization committee currently considers extending use-case options to ultra-reliable low-latency communications by enabling scheduled access along with LBT. However, this approach can increase the cost of the end systems. The aim of this study is to investigate whether standardized physical and medium access control (MAC) mechanisms, including power control, LBT, and priority queuing, can provide near-URLLC operation over multihop topologies. Our results show that to improve loss performance one needs to disable power control, use a shorter back-off window, and enable priority data transmission. For improving latency performance it is critical to use shorter acknowledgement (ACK) timeout and send ACKs immediately after data packet reception. Applying these techniques allows us to improve multi-hop URLLC latency performance by up to 30-80% and loss performance by up to 10-20% depending on URLLC and mMTC traffic conditions with only negligible impact on mMTC traffic performance.**

***Index Terms*—IoT; DECT-2020; NR+; multi-hop; URLLC.**

I. Introduction

Internet of Things (IoT) applications are becoming an integral part of our daily lives, enabling a wide range of remote functionalities from sensing to actuation [1]. Massive machine-type communications (mMTC) technologies play a pivotal role in supporting IoT. NB-IoT standardized in 3GPP Rel. 13 and then extended in subsequent releases, and LTE-M, re-branded as eMTC [2], has emerged as the standardized solution for cellular IoT (CIoT), whereas DECT-2020 NR [3] leads the way in non-cellular IoT standards.

The contemporary IoT landscape is marked by the emergence of novel applications and services that bridge the gap between URLLC and mMTC requirements. Industrial automation within factory settings, communication between unmanned aerial vehicles (UAVs), and energy grid monitoring and control exemplify this trend. These use cases demand significantly stricter latency, reliability, and throughput compared to conventional mMTC services [4]. While existing CIoT solutions such as LTE-M and NB-IoT have made strides in this direction, their inherent bandwidth limitations and shortcomings with respect to latency and reliability may hinder their ability to fully meet the stringent requirements of these emerging applications. In addition, such systems have been designed exclusively for mMTC applications and cannot multiplex traffic with strict performance requirements.

Recent studies [5], [6] demonstrated that the capacity of the recently introduced DECT-2020 system can scale up to millions of radio devices (RDs) per square kilometer while meeting the performance requirements for 5G mMTC applications outlined in [4], [7]. However, as opposed to LTE-M and NB-IoT, DECT-2020 NR is not limited to mMTC use cases. Currently, at the third evolution stage of the DECT-2020 NR specifications, the support of near-URLLC services over multi-hop topologies is investigated. Specifically, DECT-2020 adopts scheduling-based access for latency-critical traffic [8]. However, the introduction of scheduled transmissions over multi-hop topologies requires significant signaling overhead and more complex and thus more expensive end devices.

It has already been demonstrated that such services can be supported over device-to-device (D2D) links in the DECT-2020 topology with LBT access while coexisting with classic DECT systems and DECT-2020 NR operating in mMTC mode [9]. However, further improvements are needed to enable near-URLLC services in the multi-hop mode. Being aligned with 5G standards, DECT-2020 NR's physical layer offers great flexibility in physical and link layer mechanisms, including modulation and coding schemes (MCS), per-link hybrid automatic repeat request (HARQ) procedures, power control, various numerologies, etc. [10], [11]. Along with system-level solutions, such as priority queuing, these mechanisms provide a great opportunity to prioritize the traffic of URLLC applications over the air interface.

In this paper, we assess whether physical and MAC layer solutions already supported by the DECT-2020 NR standard are sufficient to enable near-URLLC services of multi-hop topologies in DECT-2020 NR systems supporting LBT access only. To this end, we first identify mechanisms that can improve the performance of near-URLLC traffic in the presence of competing mMTC traffic and then perform a detailed system-level simulation campaign that captures the specifics of medium access control and physical layer implementations.

The main contributions of this study are as follows:

- numerical comparison of various physical and MAC layer techniques for near-URLLC traffic performance in DECT-2020 NR systems with competing mMTC traffic;

- for improving loss performance of URLLC traffic by up to 10-20%, one needs to disable power control, use shorter back-off and enable priority data packet transmission at URLLC devices;
- for improving multi-hop URLLC latency performance by up two 30-80% one needs to utilize shorter acknowledgment (ACK) timeout and send ACKs immediately after data packet reception.

The remainder of this paper is organized as follows. We begin in Section II by describing the essentials of DECT-2020 NR and introducing the considered mechanisms. In Section IV, we describe the considered scenario, deployment, and system-level simulation tool. The numerical results are presented in Section V. Finally, conclusions are drawn.

II. DECT-2020 NR

In this section, we begin by describing the DECT-2020 NR basics and then introduce the mechanisms considered in this paper to enable near-URLLC communications.

A. Overall Description

The DECT-2020 NR physical layer, introduced as a set of standards in 2021, is tailored to meet current radio communication requirements [3]. It specifies 19 operational bands, the most commonly used of which are the traditional DECT bands: 1880–1900 MHz in Europe and Australia and 1900–1920 MHz in other regions. These bands accommodate up to 11 channels, each with a bandwidth of 1.728 MHz. Similar to 3GPP NR, DECT-2020 NR supports multiple numerologies with a range from 27 kHz to 216 kHz. The system employs Time Division Duplex (TDD) for managing uplink and downlink operations. Cyclic Prefix Orthogonal Frequency Division Multiplexing (CP-OFDM) with Time Division Multiple Access (TDMA) and Frequency Division Multiple Access (FDMA) for radio resource allocation. This approach to channel bandwidth, symbol length, and slot structure allows seamless coexistence between legacy DECT and DECT-2020 NR systems [12].

At the Medium Access Control (MAC) layer, RDs in DECT-2020 NR can function in either fixed (FT) mode, portable termination (PT) mode, or both simultaneously (see Fig. 1). In the FT mode, RDs serve as routers, handle local resource management, connect PT-mode RDs, and forward data to the next FT node. Both modes utilize Listen Before Talk (LBT) with a binary back-off mechanism for uplink, enabling swift medium access with a minimum sensing duration of two symbols for Random Access Channel (RACH) transmissions.

The standard employs tree topologies to streamline the routing processes. Devices operating in the PT mode connect to the most suitable RD by evaluating the link quality and announced cost, which reflects the efficiency of the route to external systems. PT-mode RDs do not maintain detailed path information and rely solely on the next-hop connectivity. Consequently, the selection of effective relay points and next-hop connections is essential to ensure optimal performance.

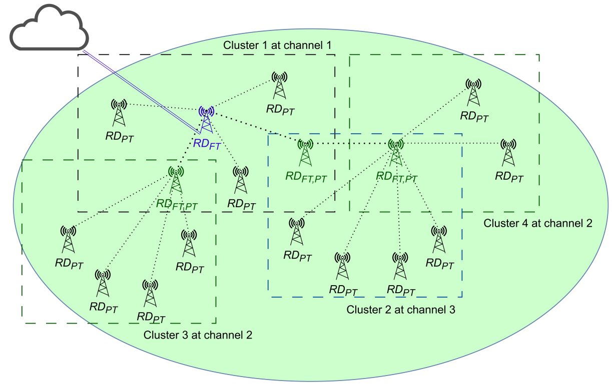

Fig. 1. Illustration of DECT-2020 network formation.

The MAC layer incorporates advanced features, such as energy conservation and power control. Energy-saving mechanisms help prolong the operational cycles of RDs, whereas power control reduces interference. When combined with tree topology, these features add layers of complexity compared with conventional CIoT systems.

B. Considered Mechanisms

There are a number of physical, link, and system-level mechanisms offered by the DECT-2020 standard even when operating in LBT channel access mode, which can be tuned to provide priorities to near-URLLC services in the presence of completing mMTC traffic.

1) LBT Mechanism: LBT mechanisms supported by DECT-2020 NR are characterized by two critical parameters affecting RD sensitivity to external interference. These are the number of symbols N sensed to detect interference and the power sensing threshold, P_{th}. As RDs in the network are not perfectly synchronized, the former may affect the packet delivery ratio (PDR) significantly. In general, the larger the value of N the better the PDR. The same applies to P_{th} as its lower values may potentially lead to better PDR. By utilizing different values of N and P_{th} one may provide implicit priority for near-URLLC traffic. In addition, making the duration of the back-off window smaller than that of the mMTC traffic may provide additional performance gains.

2) Power Control Capabilities: As DECT-2020 NR was primarily designed for mMTC applications generally characterized by a high RD density in the area, power control capabilities are a vital part of the standard. They alleviate the negative impact of interference and improve collisions as a result of LBT access. One of the potential options for providing addition prioritization at the air interface is to allow RDs transmitting packets of near-URLLC applications to utilize the full power regime, whereas mMTC packets will follow power control functionality.

3) HARQ Mechanism: DECT-2020 NR utilizes multiple modulation and coding schemes (MCS) along with a HARQ mechanism operating in the chase combining mode. The choice of a suitable MCS follows a conventional algorithm with the aim of reaching a 10% block error rate (BLER).

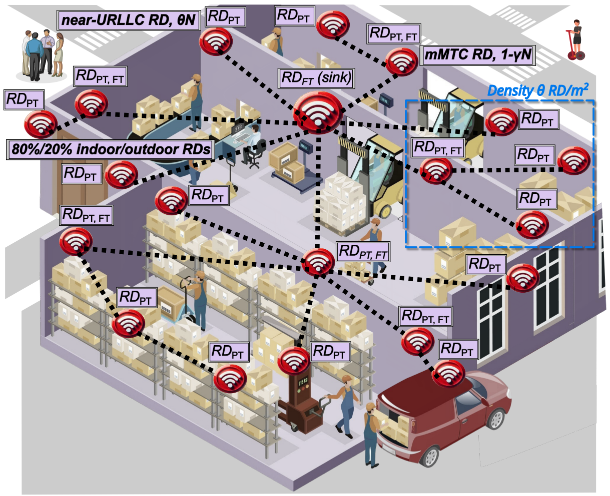

Fig. 2. An illustration of DECT-2020 NR cell deployment.

Although this is a common target for mMTC and enhanced mobile broadband (eMBB) applications, one must utilize the lowest possible MCS for near-URLLC traffic to minimize the BLER. Simultaneously, to ensure that the packet is delivered with minimal latency, one may fine-tune the HARQ operational parameters. Specifically, providing priority handling to ACK packets and sending them out immediately may improve the performance of near-URLLC applications.

4) Priority Queuing/Handling of Packets: As DECT-2020 strictly regulates only two lower levels, at the system level, one may utilize different ways to handle packets. Specifically, instead of treating all the packets equally, one may implement priority queuing for near-URLLC data packets at routers in the DECT-2020 NR network.

5) Contention Window: The contention window can be considered as yet another powerful tool to enable prioritization at the air interface. By default, all RDs in DECT-2020 compete for resources by utilizing the same maximum contention window. However, making it smaller for near-URLLC traffic can give implicit priority to channel access as compared to conventional mMTC traffic.

III. System Model

In this section, we introduce the considered system model. We begin with deployment and resources, and then specify the topology and traffic, as well as the antenna and propagation models. Finally, we introduce the considered scenarios and define the metrics of interest.

A. Deployment and Resources

We consider single-cell deployment, as illustrated in Fig. 2 with a single sink places in the center and N RDs places randomly and uniformly around in a radius of R m. The deployment of interest is a typical warehouse with walls that may affect the propagation properties and thus the multi-hop topology structure.

The system is assumed to utilize a single 1.728 MHz-wide channel in the DECT band with a carrier frequency 1.92 GHz. We assume time-division multiple access (TDMA) operational mode of the system, where the time was divided into frames of 10 ms in length. Each frame is then segmented into 10 slots, each of which can be used for LBT-based access by the RDs. We consider only the uplink RD in the sink direction.

B. Topology and Traffic

A certain fraction $\lceil \gamma N \rceil$, $\gamma \in (0,1)$ of RDs operate in routing mode, forwarding the traffic to other routers or the sink of behalf of leaf RDs. The network topology is assumed to follow a tree structure, where the successor for each node is selected based on measurements of the received signal power estimated from beacons. Beacons are always transmitted using full power. As each RD has only one path to the sink, no additional hop selection mechanism is utilized.

We assume that there are two types of multiplexed traffic in a network: mMTC traffic and near-URLLC traffic. All RDs in the system generate mMTC traffic. By following recommendations in ITU-R M.2412, the arrival process of mMTC packets is assumed to follow a homogeneous Poisson process with inter-packet time $1/\lambda_m$ s. Out of N RDs, θN, $\theta \in (0,1)$, $\theta << 1$, also run near-URLLC service. Their packets are also generated according to the Poisson process with an inter-packet time $1/\lambda_u$ s.

C. Propagation and Antenna Models

Owing to the low complexity of RDs and sink for all communicating devices, we assume single-element antennas with omnidirectional radiation patterns. The values of the receive and transmit gains, as well as the noise floor recommended in [10] are chosen, see Table II. We utilize a combination of 3GPP propagation models for the 1.9 GHz band defined in [13]. Depending on the node position, a propagation model is chosen as follows: (i) if one of the nodes is a sink, then the UMa path loss model is utilized; (ii) otherwise, if $d_{2D} < 25$, where d_{2D} is the horizontal projection distance between the interacting nodes, then the InH path loss model is used; and (iii) in the remaining cases, the UMi model is employed.

In addition, we account for line-of-sight (LoS) or non-line-of-sight (NLoS) conditions by utilizing the standardized [13] LoS blockage probabilities for UMa/UMi

$$p_L^{(U)} = \begin{cases} 1, & d_{2D} \leq 18 \\ \frac{18}{d_{2D}} + e^{-\frac{d_{2D}}{36}}(1 - \frac{18}{d_{2D}}), & 18 < d_{2D} \end{cases}, \quad (1)$$

and for inH model,

$$p_L^{(I)} = \begin{cases} 1, & d_{2D} \leq 1.2 \\ e^{-\frac{d_{2D}-1.2}{4.7}}, & 1.2 < d_{2D} < 6.5 \\ 0.32e^{-\frac{d_{2D}-6.5}{32.6}}, & 6.5 \leq d_{2D} \end{cases}. \quad (2)$$

Finally, we also account for additional building penetration losses for the UMa and UMi models if at least one node is indoors. Another loss factor is added if both nodes are indoors and $d_{2D} > 25$. The probability that any node is indoors is drawn independently as recommended in [13], i.e.,

$$PL_{pen} = 20 + 0.5U(0, 25), \quad (3)$$

TABLE I
CONSIDERED SETS OF URLLC MECHANISMS

Parameter	Priority queuing	Back-off	Power control	LBT threshold	ACK priority	LBT duration	ACK delay
Priority queuing	**Enabled**	Disabled	Disabled	Disabled	Disabled	Disabled	Disabled
Back-off	Default	**Short**	Default	Default	Default	Default	Default
Power control	Enabled	Enabled	**Disabled**	Enabled	Enabled	Enabled	Enabled
LBT threshold, dBm	- 75	-75	-75	**-100**	-75	-75	-75
ACK priority	off	off	off	off	**on**	off	off
LBT duration, symbols	2	2	2	2	2	**4**	2
ACK waiting time, slots	10	10	10	10	10	10	**1**

where $U(0, x)$ is a random sample from uniform distribution.

D. Considered Scenarios

We consider multiple scenarios. In all scenarios, the considered area of interest was of cellular form with an outer radius of 40 m and a sink located in the geometrical center at a height of 3 m. The number of RD distributed was set to 300, resulting in rather dense conditions with 0.06 devices/m^2. Some nodes generate URLLC traffic. The default system parameters are summarized in Table II. The topology construction algorithm executed at each node chooses the next hop based on the best reference signal received power (RSRP). To balance the load between routing nodes and avoid bottlebeck, we do not allow for more than 10 leafs to be associated with the routing node. The resulting topology is a tree, as dictated by the DECT-2020 NR standards. All the RDs operate in the LBT mode.

We consider multiple URLLC scenarios by varying the parameters of the mechanisms introduced in Section II-B. General system parameters as well as mMTC nodes parameters are summarized in Table II, while the specific considered URLLC cases are provided in Table I.

E. Metrics of Interest

The metrics of interest include the packet delivery ratio and and 95-percentile of latency. The latter metric shows the maximum delay experienced by 95% of RDs. We compare the resulting metrics to those standardized by ITU-R in M.2410 and M.2412 for URLLC and mMTC applications.

IV. SIMULATION TOOL

In our analysis, we capture the operation of the system at the MAC layer, including the topology construction, routing, and forwarding capabilities. Physical and MAC layer implementations follow the DECT-2020 specifications [10], [11]. However, while the MAC layer is implemented in full, the performance of the physical layer is abstracted by utilizing the BLER curves. The remaining parameters common to both systems are listed in Table II.

The DECT-2020 system was implemented using the system-level simulation tool WINTERsim, which was utilized during the standardization process of DECT-2020 technology [5]. WINTERsim is a discrete-event system-level simulation tool. For DECT-2020, we employed node abstraction as the fundamental class representing RDs. This class encapsulates all node parameters, including the position, mobility model, antenna characteristics, and power settings. Additionally, it serves as a container for Layer 2 interfaces, forwarding mechanisms, flow tables, signaling engines, application handlers, traffic generators, and physical layer interfaces. To accurately simulate high-density deployments, we implemented a physical layer abstraction that stores all bidirectional path loss states between RDs, considering only the reception signal strengths that exceed the noise floor.

The simulation process commences with node placement and path loss calculations, adhering to the 3GPP guidelines outlined in TR 38.901. Whenever feasible, we reference the ITU-R guidelines in ITU-R M.2412. To collect data, we utilized the method of replications. We conducted 25 simulation runs for each parameter set, gathering 10^5 observations in the steady state for each run. The steady-state period was identified

TABLE II
CONSIDERED SYSTEM AND EVALUATION PARAMETERS

Parameter	**Value**
General parameters	
DECT-2020 NR FT	1, height 25 m, outdoors
Carrier frequency	1900 MHz
Number of RDs	100
Fraction of URLLC RDs	0.1
Number of channels	1
Channel bandwidth	1.728 MHz
RD deployment	Uniformly random
Building penetration loss	20 dB (ITU-R)
Indoor/outdoor fraction	80% / 20%
Channel model, Sink-Node	Urban macro
Channel model, Node-Node	Urban street canyon
Number of node/sink antenna elements	1
Sink/RD noise figure	7 dB
Sink/RD antenna element gain	0 dBi
Thermal noise level	–174 dBm/Hz
Traffic model	Bursts of 2 packets
Application data message size	32 bytes
Channel access	LBT
Contention window size	min – 24, max – 768
Rx sensitivity	-99.7 dBm (TS 103.636-2)
Max Tx power	10 dBm
Format	MSC 1,3,4 (1,2,3 packets)
URLLC inter-arrival time	fixed, 8 ms, 16 ms
mMTC RD parameters	
Mean inter-arrival time	10-50 s
Inter-arrival time distribution	Exponential
LBT threshold	-75 dBm
Error correction	HARQ with 3 attempts
Power control	Enabled
LBT sensing duration	2 symbols
ACK waiting time	10 slots

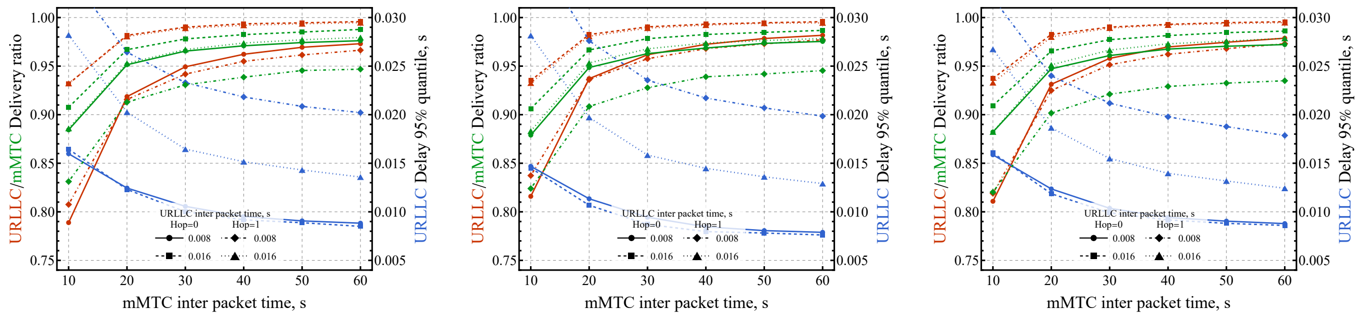

(a) Priority queuing (b) Shorter back-off (c) ACK priority

Fig. 3. Performance of MAC layer mechanisms: priority queuing for data and ACK packets and shorted back-off window.

using moving average statistics. Owing to the substantial size of the statistical samples, we present only point estimates.

V. Numerical Results

In this section, we report our numerical results. We begin with the baseline scenario, where both considered traffic types are handled the same way and then proceed to address the URLLC candidate cases defined in Table II. We present near-URLLC latency performance only as in all considered experiments mMTC latency performance satisfied ITU-R guidelines specified in M.2410 and M.2412, i.e., was less than 10 s.

A. Baseline Performance

We begin with the baseline performance, when URLLC RD parameters coincide with those of mMTC RDs, and the only difference is the packet generation rate. For this case, the PDR and 95-th latency quantile for URLLC and mMTC traffic are presented in Fig. 4. Note that we show URLLC performance for both single-hop communications when RD is directly connected to the sink, and for multi-hop communications, where there is at least one relaying point between URLLC RD and the sink.

By analyzing the presented results, one first observes that there is a principle difference between single- and multi-hop URLLC performance in terms of both investigated metrics. For the single-hop case and a small load of mMTC traffic (40-60 s between packet arrivals at mMTC RDs), PDR is perfect for the single-hop case, whereas it stays at approximately 0.97-0.98 for the multi-hop cases. The increase in the traffic rate from URLLC RDs has a similar impact. In terms of latency quantile, we observe that single-hop communications with a 16 ms interval between URLLC packet generation results in a respectable 15 ms latency quantile for single-hop communications. However, switching to multi-hop mode leads to doubling of the latency quantile while increasing the traffic rate two times adds comparable latency on top of that. In the following discussion, we mainly concentrate on performance improvements for URLLC multi-hop communications.

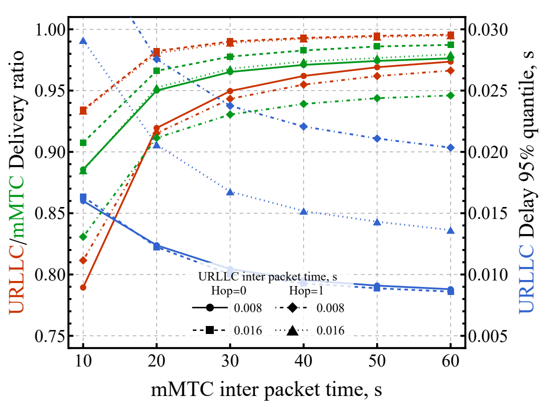

Fig. 4. URLLC and mMTC RDs performance or baseline scenario.

B. Mechanisms in Isolation

We now assess the impact of the MAC and physical mechanisms summarized in Table I in isolation. We begin with a performance analysis of MAC layer mechanisms, including priority queuing, utilizing shorter backoffs, and enabling ACK priority handling for URLLC packets in Fig. 3. By analyzing the presented results, we observe that enabling priority queuing provides gains on the order of 2-3% for in terms of both PDR and latency performance. Utilizing a shorter back-off window is more impactful, especially for single-hop operations, for example, 95% packet latency decreases from 17 ms to 14 ms for the smallest considered mMTC inter-packet generation time. The highest impact on multi-hop URLLC performance is produced by ACK priority handling, where a notable reduction in the 95% latency quantile is observed. This mechanism also improves the PDR performance by 2-3%.

Now, consider the impact of the physical layer mechanisms shown in Fig. 5. Here, we observe that disabling power control at URLLC RDs leads to a drastic improvement in PDR performance. Specifically, even for the small mMTC inter-packet generation time and 16 ms URLLC inter-packet generation time, the PDR is still at 0.99, as compared to the baseline when it is just 0.93. Similar improvements were observed for other traffic loads. The associated 95% quantile performance, however, improves for the single-hop scenario only, but the gain is drastic and may reach 30%. In contrast, the utilization of a lower LBT threshold and longer LBT sensing duration (four instead of just two symbols) worsens the PDR and latency performance.

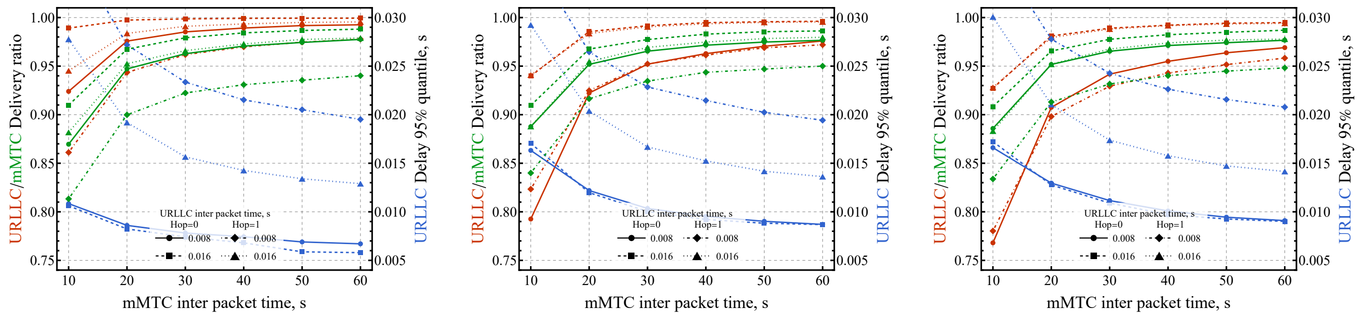

(a) No power control

(b) Lower LBT threshold

(c) Longer LBT duration

Fig. 5. Impact of physical layer mechanisms: power control, LBT threshold and its duration.

In summary, we conclude that disabling power control for URLLC RDs is the most effective way to improve the latency and PDR performance. Utilizing priority queuing, shorter back-off window, and sending ACK packets immediately also positively affect URLLC traffic performance. However, having a smaller LBT threshold and larger LBT sensing duration makes URLLC RDs more hesitant to transmit packets, thus negatively affecting the performance metrics of interest.

C. Selected Candidate Schemes

Having studied the system's response to individual mechanisms, we now consider two selected schemes that are shown to provide the biggest performance boost to URLLC RDs. The first scheme, the performance of which is shown in Fig. 6(a), assumes no power control, but utilizes shorter back-off timer and priority queuing. By cross-comparing the presented results to those shown for the baseline scheme in Fig. 4, we observe that the reliability region of the system is significantly extended as PDR remains close to one over the whole considered mMTC traffic parameters for single-hop communications and 16 ms interarrival time between URLLC packets. The performance of the multi-hop case is also improved, and now PDR is close to 1 for 16 ms URLLC interval time for 30-60 s interarrival arrival time between mMTC packets. Comparable improvements are observed with respect to the latency quantile performance, which is now less than 10 ms for single-hop communications for the higher considered mMTC traffic load. Latency quantile performance is also drastically improved in the case of multi-hop communications, especially for high mMTC load conditions.

The second identified candidate case features all those mechanisms selected for the first case and also adds immediate ACK for transmitted URLLC packets and also utilizes shorter ACK timeout, see Fig. 6(b). The major impact is logically observed for the latency quantiles. Specifically, even for multihop communications under the worst possible URLLC and mMTC traffic conditions, it is now smaller than 30 ms. At the same time, the PDR performance does not degrade significantly as compared to Fig. 6(a). By cross-comparing Figs. 6 and Fig. 4, the performance degradation of mMTC traffic is negligible.

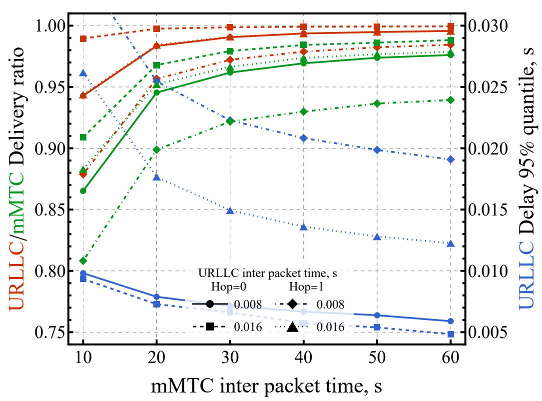

(a) No power control, short back-off, priorities

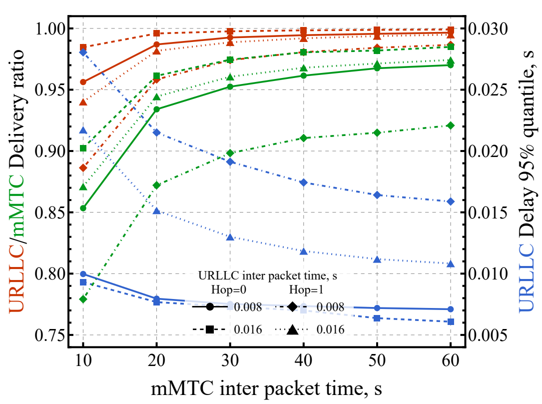

(b) No power control, short back-off, priorities, immediate ACK

Fig. 6. Performance of selected sets of mechanisms.

VI. Conclusions

The market for small data communications is characterized by the appearance of applications having requirements in-between conventional mMTC and URLLC services, so-called near-URLLC applications. Motivated by the need to support such applications in DECT-2020 NR LBT-based technology, in this study, we analyzed the impact of various physical and MAC layer mechanisms on the performance of near-URLLC traffic in the presence of competing mMTC traffic.

Our results show that there are two groups of mechanisms that affect the loss and latency performance of URLLC traffic. Disabling power control, utilizing a shorter than default back-off window, and enabling priority data packets queuing ar

URLLC RDs are critical for improving loss performance. The gains in terms of PDR may reach 10-20% as compared to the baseline. Using a shorter ACK timeout and prioritized transmission of ACKs at URLLC RDs are essential for providing better latency performance with gains in terms of 95% quantile latency reaching 30-80%. Notably, the associated performance degradation of mMTC traffic is negligible.

We note that anything beyond the reported reliability and latency performance requires the use of DECT-2020 NR scheduling-based MAC, which is characterized by more complicated protocol logic and associated signaling overheads.

ACKNOWLEDGMENT

This work was supported by the CELTIC-NEXT "Ultra Scalable Wireless Access" (USWA) project.

REFERENCES

[1] A. Khanna and S. Kaur, "Internet of things (iot), applications and challenges: a comprehensive review," *Wireless Personal Communications*, vol. 114, no. 2, pp. 1687–1762, 2020.

[2] H. Fattah, *5G LTE Narrowband Internet of Things (NB-IoT)*. CRC Press, 2018.

[3] ETSI, "DECT-2020 New Radio (NR); Part 1: Overview," ETSI, TS 103 636-1 v1.3.1, December 2021.

[4] ITU-R, "Minimum requirements related to technical performance for IMT-2020 radio interface," ITU-R, M.2410-0, July 2017.

[5] R. Kovalchukov, D. Moltchanov, J. Pirskanen, J. Säe, J. Numminen, Y. Koucheryavy, and M. Valkama, "DECT-2020 New Radio: The Next Step toward 5G Massive Machine-Type Communications," *IEEE Communications Magazine*, vol. 60, no. 6, pp. 58–64, 2022.

[6] A. Anttonen, P. Karhula, M. Lasanen, and M. Majanen, "Enabling Massive Machine Type Communications with DECT-2020 Standard: A System-Level Performance Study," *VTT Technical Research Centre of Finland*, 2021.

[7] ITU-R, "Guidelines for evaluation of radio interface technologies for IMT-2020," ITU-R, M.2412-0, July 2017.

[8] ETSI, "DECT-2020 New Radio (NR); Part 4: MAC layer; Release 1," ETSI, TS 103 636-4 v1.3.1, December 2021.

[9] A. Samuylov, D. Moltchanov, A. Gaydamaka, E. Lyczkowski, A. Frotzscher, F. von Schoettler, J. Pirskanen, J. Numminen, J. Salokannel, E. Llaguno, R. Pires, D. Bayar, and M. Valkama, "Empowering Near-URLLC IoT with 5G DECT-2020 NR: Current State and the Road Ahead," *IEEE Communications Magazine*, vol. 1, no. 1, pp. 1–6, 2025.

[10] ETSI, "DECT-2020 New Radio (NR); Part 2: Radio reception and transmission requirements; Release 1," ETSI, TS 103 636-2 v1.3.1, December 2021.

[11] ——, "DECT-2020 New Radio (NR); Part 3: Physical layer; Release 1," ETSI, TS 103 636-3 v1.3.1, December 2021.

[12] A. Samuylov, D. Moltchanov, J. Pirskanen, J. Numminen, Y. Koucheryavy, and M. Valkama, "Performance assessment of dect-2020 nr and classic dect coexistence mechanisms," in *2023 IEEE 97th Vehicular Technology Conference (VTC2023-Spring)*. IEEE, 2023, pp. 1–7.

[13] 3GPP, "Study on channel model for frequencies from 0.5 to 100 GHz (Release 14)," 3rd Generation Partnership Project (3GPP), 3GPP TR 38.901 V14.1.1, July 2017.